High-T_c Spin Superfluidity in Antiferromagnets

Yu. M. Bunkov,[1] E. M. Alakshin,[2] R. R. Gazizulin,[2] A. V. Klochkov,[2] V. V. Kuzmin,[2] V. S. L'vov,[3] and M. S. Tagirov[2]

[1]*Institute Neel, CNRS, Grenoble, 30842, France*
[2]*Kazan Federal University, Kazan, 420008, Russia*
[3]*The Weizmann Institute of Science, Rehovot, 76100, Israel*

(Received 31 October 2011; published 23 April 2012)

We report the observation of the unusual behavior of induction decay signals in antiferromagnetic monocrystals with Suhl-Nakamura interactions. The signals show the formation of the Bose-Einstein condensation (BEC) of magnons and the existence of spin supercurrent, in complete analogy with the spin superfluidity in the superfluid ^{3}He and the atomic BEC of quantum gases. In the experiments described here, the temperature of the magnon BEC is a thousand times larger than in the superfluid ^{3}He. It opens a possibility to apply the spin supercurrent for various magnetic spintronics applications.

DOI: 10.1103/PhysRevLett.108.177002 PACS numbers: 74.70.Tx, 74.25.Ha, 75.20.Hr

Predicted in 1925 by Einstein for bosonic particles (see, e.g., [1]), the Bose-Einstein condensation (BEC) corresponds to the formation of a collective quantum state in which a macroscopic number of particles is governed by a single wave function. Almost perfect BEC states were observed in ultracold atomic gases. In Bose liquids, the BEC is strongly modified by interactions; however, it still remains the key mechanism for the formation of a coherent quantum state experiencing the phenomenon of superfluidity, i.e., the existence of a nondissipative superfluid current. Both BEC and superfluidity do not require a strict conservation of the number of particles but might be observed as well when this conservation law is weakly violated [for example, in systems of such sufficiently long-lived quasiparticles as phonons, rotons, spin waves (magnons), excitons, etc.] [2].

The phenomenon of magnon BEC was described by Bunkov and Volovik [3,4] to explain the long-term spin dynamics in the superfluid ^{3}He. The magnon BEC is a direct magnetic analogy with an atomic BEC. It manifests itself by a phase-coherent precession of magnetization (even for an inhomogeneous static magnetic field) which was discovered in the superfluid ^{3}He-B [5]. In a BEC state, the transverse component of the magnetization is described by a wave function $S_\perp \exp(i\omega t + \phi)$ which expresses all the properties of the spin superfluidity. The spatial gradient of the phase ϕ leads to a spin supercurrent which transports the magnetization. Some of the experimental observations consist of phase-slip processes at the critical current [6], Josephson spin-current effects [7], as well as spin-current vortices [8], etc. A comprehensive review can be found in [9], while there are more recent ones in [10,11]. From experiments carried out with ^{3}He, it becomes clear that the spin superfluidity is not a consequence of the mass superfluidity. The spin superfluidity is related to a particular magnetic interaction. That is why finding new classes of materials with specific magnetic interaction is a prospective project in terms of observing solely the spin superfluidity [12]. In the present Letter, we report the first experimental confirmation of magnon BEC in easy-plain antiferromagnets (AFMs) $CsMnF_3$ and $MnCO_3$ with a strong nuclear-electron interaction. Their Neel temperatures are 55 and 32 K, respectively. Our experiments were carried out at 1.5 and 4.2 K. At these temperatures, the magnons are well-defined quasiparticles. The previous experiments were made in the superfluid ^{3}He with the Neel temperature equal to a superfluid transition temperature of about 1 mK.

$CsMnF_3$ and $MnCO_3$ are AFMs with the Suhl-Nakamura interaction [13], which is an indirect nuclear-nuclear exchange interaction through magnetically ordered electrons. The nuclear magnetic resonance (NMR) frequency of ^{55}Mn ω^{n0} is very high, about 600 MHz, while the electron AFM resonance frequency ω^{e0} in easy-plane and cubic AFMs might be very low in the presence of a small external magnetic field H_0. These "bare" frequencies are modified into ω^n and ω^e by the hyperfine interaction frequencies as follows:

$$\omega^e = \sqrt{(\omega^{e0})^2 + (\omega^e_{\rm hf})^2}, \qquad \omega^{e0} = \gamma_e\sqrt{H_0(H_0 + H_D)},$$
$$\omega^e_{\rm hf} = \gamma_e H^e_{\rm hf}, \qquad H^e_{\rm hf} = A\gamma_e m_z, \tag{1a}$$

$$\omega^n_k(\beta) = \omega^{n0} - \frac{\omega_p(\beta)}{1 + (kr_0)^2}, \qquad \omega^{n0} = \gamma_n(H_0 + H^n_{\rm hf}),$$
$$\omega_p(\beta) = \omega^{n0}\frac{H_{\rm ex}H^e_{\rm hf}}{2H^2}\frac{m\cos\beta}{M}, \qquad H^n_{\rm hf} = A\gamma_n M. \tag{1b}$$

Here, γ_e and γ_n are the gyromagnetic ratios for electrons and for the ^{55}Mn nuclei, respectively; H_0 is the external field; H_D is the so-called Dzyaloshinsky magnetic field ($H_D \simeq 4.4$ kOe in $MnCO_3$ and zero in $CsMnF_3$); $H^e_{\rm hf}$ and $H^n_{\rm hf}$ are the hyperfine magnetic fields on the electron and nuclear sublattices; A is the hyperfine constant; $M \equiv |\boldsymbol{M}|$ and $m \equiv |\boldsymbol{m}|$ are the electron and nuclear magnetizations; and β is the angle of nuclear magnetization deflection (1b). Finally, r_0 is a Suhl-Nakamura interaction radius (about

10^4 interatomic distances for the AFMs discussed here), which originates from a stiffness of the magnetically ordered electrons.

Note that, in the electron AFM resonance frequency (1a), ω^e, there is a hyperfine gap $\omega_{\rm hf}$ even for $H_0 = 0$. The nuclear magnon frequency (1b), $\omega_k^n(k)$, experiences a shift-down in frequency, denoted by ω_p, which can be referred to as "pulling" [14]. For such easy-plane AFMs as $CsMnF_3$, this pulling frequency ω_p satisfies Eq. (1b). For such weak ferromagnets as $MnCO_3$, the dependence is more complicated [15]. Note that Eq. (1b) also describes a positive dynamical frequency shift—a nonlinear dependence of $\omega_k^n(\beta)$ on the level of the system excitation characterized by the deflection angle β. The pulling frequency ω_p, entering into Eq. (1b) with negative sign, decreases while the amplitude of homogeneous precession β increases. Notice also that, for nuclear magnetic excitations with $kr_0 \gg 1$ (meaning $\omega_k^n(k) \to \omega^{n0}$), statistical correlations of neighboring nuclear magnetic moments are lost and therefore those excitations cannot be considered as collective motions or magnons.

The above-described nuclear spin system in easy-plane AFMs shows many similarities with the superfluid ^{3}He-A [16], particularly if the orbital momentum of ^{3}He-A is directed along the magnetic field [17,18]. In both of these cases, the frequency of long-wave magnons includes positive and quadratic contributions $\delta\omega_k \propto k^2$ as well as a certain increase of the nonlinear frequency shift with the level of excitation (due to the repulsive interaction between magnons). Taking into account that the magnon BEC in ^{3}He-A was observed under continuous wave NMR conditions [19,20], we performed similar experiments in $CsMnF_3$ and observed indeed very similar results [21]. These experiments cannot be considered as a solid confirmation of the BEC because the continuous wave NMR data can also be interpreted in terms of nonlinear magnetic resonance in samples with a dynamical frequency shift. For a certain confirmation, we need to investigate the free induction decay (FID) radiated by the BEC state as it was performed in ^{3}He-A [20].

The experiments were carried out at the temperature of 1.5 K. The sample (it was a single crystal of the volume of about a few mm^3) was placed inside the split-ring resonator [22] tuned to the frequency $\omega_{\rm rf} = 566.7$ MHz with $Q = 150$. Complete details of the experimental setup will be discussed elsewhere. We applied rf pulses (homogeneous on the scale of the sample) of various amplitudes with frequencies $\omega_{\rm rf}$, which were either at least equal to or higher than the resonant NMR frequency $\omega_k^n(0)$. We achieved this difference by changing the value of the external magnetic field according to Eq. (1b). Surprisingly, FID was observed not only at the resonant condition but also at far higher rf frequencies $\omega_{\rm rf}$, provided that the rf signal was both intensive enough and long enough. The left panel of Fig. 1 depicts the amplitude of the FID just after switching off the rf field as a function of the rf pulse length. For short rf pulses of about 0.01 ms, we clearly saw FID of large amplitude at magnetic fields of about 455 mT. That gave us the NMR resonance frequency for $\simeq 565.8$ MHz for $\beta = 0$.

After applying the pulse, the frequency of induction changes up to the frequency of the resonator 566.7 MHz. We have calibrated the signal (in units of the angle β of the full magnetization deflection) after short pulses by fitting the amplitude for different frequency shifts. The procedure of fitting is to be published elsewhere. By decreasing the value of H, the resonance frequency moves down as well and the amplitude of the FID after a few short pulses decreases as expected and, finally, disappears completely at $B_0 = 445$ mT. Nevertheless, the FID appears if the length of the rf pulse increases. For example, we lowered down the B_0 field to 433 mT, meaning that $\omega_0^n(0) = 557.8$ MHz (which stands far outside the resonance conditions), and we observed a FID after a long rf pulse (about

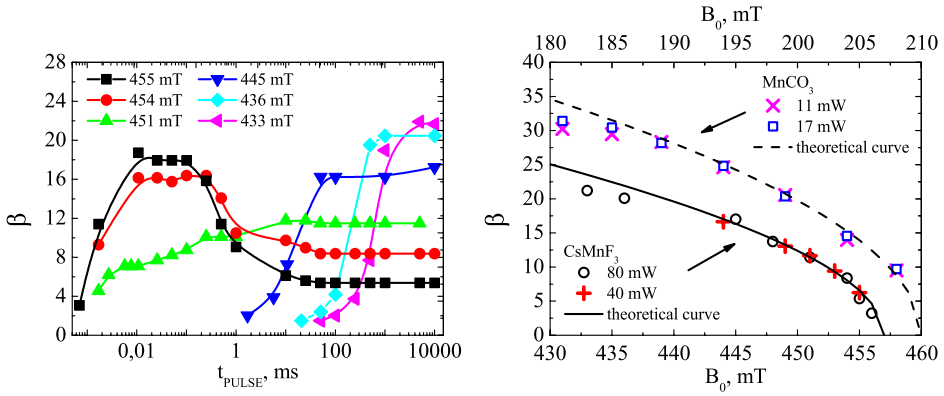

FIG. 1 (color online). Left: The amplitude of free induction decay (in units of magnetization deflection β) as a function of a length of the rf pulse for different external magnetic fields in $CsMnF_3$. Right: The amplitude of FID after a 10 s pulse in $CsMnF_3$ (bottom axis of fields) and $MnCO_3$ (top axis of fields) as a function of the external magnetic field for two different rf field energies. The solid (for $CsMnF_3$) and dashed (for $MnCO_3$) black lines show the theoretical curve (3) which corresponds to the conditions of BEC formation.

10 s) whose amplitude was surprisingly huge. Note that, if the nuclear magnetization thermalizes, as was traditionally suggested, we would not have been able to see any induction signal except that one at the resonance conditions and for short pulses. Instead of this, our observations possess a natural explanation within the framework of the theory of magnon BEC, as we will describe below. Briefly, the BEC of magnons is created during the long and intensive nonresonant rf field. The rf field pumps the magnons with nonzero k whose frequency $\omega_k^n(0)$ corresponds to the $\omega_{\rm rf}$. The pulling decreases due to the repulsive interaction between magnons. Finally, all magnons condensate to a minimum of energy in a rotating frame, where $\omega_0^n(\beta) = \omega_{\rm rf}$. It is clear that larger initial frequency differences require a longer rf pumping time in order to collect enough magnons to provide the needed frequency shift. In Fig. 1 (right), the amplitude of FID after a long pulse is shown as a function of the magnetic field. A larger initial frequency difference enlarges the FID, whose amplitude corresponded well to the angle β for the conditions of BEC formation on a given frequency and field, as we shall describe later. From this observation, we can conclude that the above-described long-pulse NMR experiments give us the solid confirmation of magnon BEC.

As in the case of the atomic BEC, the essential physical picture of the magnon BEC can be described by the Ginzburg-Landau free energy functional $\mathcal{F}$ which (in the reference frame rotating with the rf frequency $\omega_{\rm rf}$) is given by [4]

$$\mathcal{F} = \int d^3r \left\{ \frac{|\nabla\Psi|^2}{2m_M} + [\omega_k^n - \omega_{\rm rf}]|\Psi|^2 + \frac{b}{2}|\Psi|^4 \right\}. \quad (2)$$

For magnon systems, the complex order parameter $\Psi(\boldsymbol{r}, t)$ is the vacuum expectation value of the magnon field operator $\hat{\Psi}(\boldsymbol{r}, t)$: $\Psi(\boldsymbol{r}, t) = \langle\hat{\Psi}(\boldsymbol{r}, t)\rangle$. For homogeneous precession, the magnon number density n can be related to the deflection angle β via $n = |\Psi|^2 = m(1 - \cos\beta)$. The first term in the integrand (2) describes the kinetic energy of magnons with the effective mass $m_M = 2/\omega_p r_0^2$. The resonance frequency of homogeneous ($k = 0$), low-amplitude ($\beta = 0$) NMR, $\omega_k^n \equiv \omega_k^n(0, 0) = \omega^{n0} - \omega_p(0)$, plays the role of an external potential in atomic condensates. The last term with $b = \omega_p/m$, originating from the β dependence of $\omega_p(\beta)$ in Eq. (1b), describes the dynamical frequency shift up and, within Eq. (2), can be interpreted as a self-similar nonlinear contribution to the potential energy of magnons due to their repulsion.

From a thermodynamical viewpoint, given a value of $\omega_{\rm rf}$, the system of interacting magnons tends to evolve toward the thermodynamic equilibrium with minimal free energy (2). This minimum is reached at $\nabla\Psi = \mathbf{0}$ (i.e., for homogeneous excitation—magnons with $k = 0$) and for $b|\Psi|^2 = \omega_{\rm rf} - \omega_k^n$. This can be identically rewritten as a condition of homogeneous nonlinear NMR:

$$\omega_{\rm rf} = \omega_0^n(\beta) = \omega^{n0} - \omega_p(0)\cos\beta. \quad (3)$$

We have found that this condition corresponds exactly to the experimental results, as shown in Fig. 1 (right).

Understanding how the thermodynamic equilibrium (3) can be reached requires a more detailed description of the system. For simplicity, we restrict ourselves to the classical limit and consider a Hamiltonian function $\mathcal{H}$ of imperfect AFM in an external rf field $h(t) = h\exp(i\omega_{\rm rf}t)$. In the laboratory reference frame and in the $\boldsymbol{k}$ representation,

$$\mathcal{H} = \sum_{\boldsymbol{k}} \omega_k^n a_{\boldsymbol{k}} a_{\boldsymbol{k}}^* + \mathcal{H}_{\rm rf} + \mathcal{H}_{\rm def} + \mathcal{H}_{\rm int}, \quad \omega_k^n \equiv \omega_k^n(0), \quad (4a)$$

$$\mathcal{H}_{\rm rf} = \sum_{\boldsymbol{k}} [h(t)V_k a_{\boldsymbol{k}} + \text{c.c}], \quad \mathcal{H}_{\rm def} = \sum_{\boldsymbol{k},\boldsymbol{k}'} \tilde{g}_{\boldsymbol{k},\boldsymbol{k}'} a_{\boldsymbol{k}} a_{\boldsymbol{k}'}^*, \quad (4b)$$

$$\mathcal{H}_{\rm int} = \frac{1}{4} \sum_{\boldsymbol{k}_1+\boldsymbol{k}_2=\boldsymbol{k}_3+\boldsymbol{k}_4} T_{\boldsymbol{k}_1,\boldsymbol{k}_2,\boldsymbol{k}_3,\boldsymbol{k}_4} a_1^* a_2^* a_3 a_4, \quad a_j \equiv a_{\boldsymbol{k}_j}. \quad (4c)$$

Here, $a_{\boldsymbol{k}} = \int \Psi(\boldsymbol{r})\exp(i\boldsymbol{k}\cdot\boldsymbol{r})d\boldsymbol{r}/\int d\boldsymbol{r}$ denotes the canonical amplitude of the magnons. The Hamiltonian $\mathcal{H}_{\rm def}$ describes the elastic two-magnon scattering on random inhomogeneities; for small defects of volume v_0 that are randomly distributed at positions $\boldsymbol{r}_n$, we find $\tilde{g}_{\boldsymbol{k},\boldsymbol{k}'} = v_0 g_{\boldsymbol{k},\boldsymbol{k}'} \sum_n \exp[i(\boldsymbol{k} - \boldsymbol{k}')\cdot\boldsymbol{r}_n]$, where $g_{\boldsymbol{k},\boldsymbol{k}'}$ is the scattering amplitude on an individual defect; $\mathcal{H}_{\rm int}$ is responsible for $(2 \Leftrightarrow 2)$ magnon scattering. From Eqs. (1b), one can readily evaluate that, in the region $k \lesssim 1/r_0$, the amplitude of the interaction is $T(\boldsymbol{k}_1, \boldsymbol{k}_2, \boldsymbol{k}_3, \boldsymbol{k}_4) \sim b$.

Using the Hamiltonian (4), one can write the kinetic equation

$$\dot{n}_k \equiv \frac{dn_k}{dt} = \mathrm{St}_{\boldsymbol{k}}^{\rm def} + \mathrm{St}_{\boldsymbol{k}}^{\rm int}, \quad (5)$$

where St are collision integrals defined as

$$\mathrm{St}_{\boldsymbol{k}}^{\rm def} = \pi C \int |g_{\boldsymbol{k},\boldsymbol{k}'}|^2 (n_{\boldsymbol{k}'} - n_{\boldsymbol{k}}) \delta[\omega_k^n(k) - \omega_k^n(k')],$$

$$\mathrm{St}_{\boldsymbol{k}}^{\rm int} = \pi \int |T_{\boldsymbol{k},\boldsymbol{k}_1,\boldsymbol{k}_2,\boldsymbol{k}_3}|^2 n_{\boldsymbol{k}} n_1 n_2 n_3 \left[\frac{1}{n_{\boldsymbol{k}}} + \frac{1}{n_1} - \frac{1}{n_2} - \frac{1}{n_3}\right] \times \delta(\omega_k^n + \omega_1^n - \omega_2^n - \omega_3^n) \times \delta(\boldsymbol{k} + \boldsymbol{k}_1 - \boldsymbol{k}_2 - \boldsymbol{k}_3) d\boldsymbol{k}_1 d\boldsymbol{k}_2 d\boldsymbol{k}_3.$$

Here, C is the concentration of defects. In the presence of an intense rf field, the role of $n_{\boldsymbol{k}'}$ is played by the forced homogeneous precession: $n_{\boldsymbol{k}'} = \mathcal{N}_0 \delta^3(\boldsymbol{k}')$, $\omega_k^n(k') \Rightarrow \omega_{\rm rf}$, and the term $\propto n_{\boldsymbol{k}}$ in $\mathrm{St}_k^{\rm def}$ can be neglected, compared to the term $\propto n_{\boldsymbol{k}'}$. Then, Eqs. (5) give for the pumping rate of the total number of magnons $N_{\tilde{k}} \equiv \int n_k d\boldsymbol{k}$, with wave vectors $|\boldsymbol{k}| \equiv \tilde{k}$ defined by the resonance condition $\omega_{\rm rf} = \omega_{\tilde{k}}^n$:

$$\dot{N}_{\tilde{k}} = \gamma_{\rm def}(\tilde{k})\mathcal{N}_0, \qquad \gamma_{\rm def}(k) \equiv (2\pi)^2 C \frac{|g_{0,k}|^2 k^2}{d\omega_k^n/dk}. \quad (6)$$

Notice that $\mathrm{St}_k^{\mathrm{int}}$ does not contribute to $dN(t)/dt$, thereby ensuring the conservation of $N(t)$ and of the total energy $E(t) = \int \omega_k^n n_k d^3\boldsymbol{k}$.

It is known from the theory of weak wave turbulence [23] that the scattering (4c) results mostly in a flux of energy toward large k which leads to an accumulation of energy at large k with some rate $\dot{E}_\infty$ and to a flux of particle number toward small k which leads to an accumulation of particles at small k with a rate $\dot{N}_0$. In our system, the overall particle number and energy balance in the stationary case can be written as follows:

$$\dot{N} = \dot{N}_0 + \dot{N}_\infty, \qquad \dot{E} = \dot{E}_0 + \dot{E}_\infty, \tag{7a}$$

$$\dot{E} = \omega_{\mathrm{rf}}\dot{N}, \qquad \dot{E}_0 = \omega_0^n \dot{N}_0, \qquad \dot{E}_\infty \simeq \omega^{n0}\dot{N}_\infty. \tag{7b}$$

The relation between $\dot{E}$ and $\dot{N}$ follows from the fact that the pumping of N and E (due to elastic scattering on inhomogeneities) is located at a fixed frequency ω_{rf}. The time derivatives $\dot{E}_0$ and $\dot{N}_0$ are connected to each other via the frequency of homogeneous precession ω_0^n, and the estimation for $\dot{E}_\infty$ follows from the fact that the main contribution to the large k energy is dominated by the region $k \ll 1/r_0$, where $\omega_k^n \simeq \omega^{n0}$.

The solution of (7) [with a substitution of $\dot{N}_0$ from (6)] is

$$\dot{N}_0 \simeq \gamma_{\mathrm{def}} \mathcal{N}_0 [\omega^{no} - \omega_{\mathrm{rf}}]/\omega_p(\beta), \tag{8a}$$

$$\dot{E}_\infty \simeq \gamma_{\mathrm{def}} \mathcal{N}_0 \omega^{no} [\omega_{\mathrm{rf}} - \omega^{no} + \omega^p(\beta)]/\omega_p(\beta). \tag{8b}$$

Equation (8a) describes the rate of BEC of magnons at $k = 0$, i.e., the growth of a homogeneous precession of magnetic moment with a frequency ω_0^n. Equation (8b) shows the heating rate of the thermostat of thermal magnons. This effect can be totally neglected at experimental temperatures. It means that the magnetization m must remain practically constant, even though $\cos\beta$ does decrease with time (linearly, in the beginning of rf pumping).

The challenge can be stated as follows: "Does the true magnon BEC, accompanied by all its usual features, including spin supercurrent, actually exist in AFMs?" The samples are inhomogeneous. The characteristic inhomogeneity frequency $\Delta\omega^{n0}$ is about 2 MHz, which is much smaller than the pulling frequency ω_p. In this case, the nuclear spins should precess coherently only on a scale of the approximate interaction radius r_0. The effective intensity of the rf field was only about 300 kHz and cannot suppress the inhomogeneity on a long distance. Nevertheless, we observed the FID signal whose amplitude corresponds to a homogeneous precession of full magnetization, deflected on the angle β in complete agreement with the theory of magnon BEC (Fig. 1). We consider this as evidence of the spin supercurrent—an essential feature of the BEC which redistributes the longitudinal magnetization to compensate the inhomogeneity of the precession.

The BEC of magnons with $k \neq 0$ was observed by optical methods in ferromagnetic yttrium-iron garnet [24]. In this case, the state with $k \neq 0$ corresponds to a minimum of potential, and therefore BEC is possible. Indeed, the state should be very interesting, since optically the two BEC states with k and $-k$ were observed. It is possible that this state can be similar to a charge-density wave of electrons.

We are grateful to Laurent Boué for useful comments on the manuscript. This work is partly supported by the Ministry of Education and Science of the Russian Federation (FTP "Scientific and scientific-pedagogical personnel of the innovative Russia" Contract No. N02.740.11.5217), by the EU-FP7 program (N228464 Microkelvin), and by the CNRS—Russian Academy of Science collaboration (N16569).

[1] S. Giorgini, L. P. Pitaevskii, and S. Stringari, Rev. Mod. Phys. **80**, 1215 (2008).
[2] D. Snoke, Nature (London) **443**, 403 (2006).
[3] Yu. M. Bunkov and G. E. Volovik, Phys. Rev. Lett. **98**, 265302 (2007).
[4] Yu. M. Bunkov and G. E. Volovik, J. Low Temp. Phys. **150**, 135 (2007).
[5] A. S. Borovik-Romanov, Yu. M. Bunkov, V. V. Dmitriev, and Yu. M. Mukharskiy, JETP Lett. **40**, 1033 (1984); I. A. Fomin, *ibid.* **40**, 1037 (1984).
[6] A. S. Borovik-Romanov, Yu. M. Bunkov, V. V. Dmitriev, Yu. M. Mukharskiy, and D. A. Sergatskov, Phys. Rev. Lett. **62**, 1631 (1989).
[7] A. S. Borovik-Romanov, Yu. M. Bunkov, A. de Waard, V. V. Dmitriev, V. Makrotsieva, Yu. M. Mukharskiy, and D. A. Sergatskov, JETP Lett. **47**, 478 (1988).
[8] A. S. Borovik-Romanov, Yu. M. Bunkov, V. V. Dmitriev, Yu. M. Mukharskiy, and D. A. Sergatskov, Physica (Amsterdam) **165B**, 649 (1990).
[9] Yu. M. Bunkov, J. Low Temp. Phys. **135**, 337 (2004); Prog. Low Temp. Phys. **14**, 69 (1995).
[10] Yu. M. Bunkov and G. E. Volovik, J. Phys. Condens. Matter **22**, 164210 (2010).
[11] Yu. M. Bunkov, J. Phys. Condens. Matter **21**, 164201 (2009).
[12] V. P. Mineev, JETP **83**, 1217 (1996).
[13] H. Suhl, Phys. Rev. **109**, 606 (1958); T. Nakamura, Prog. Theor. Phys. **20**, 542 (1958).
[14] A. S. Borovik-Romanov, Yu. M. Bunkov, and B. S. Dumesh, Physica (Amsterdam) **86B+C**, 1301 (1977).
[15] A. S. Borovik-Romanov, Yu. M. Bunkov, B. S. Dumesh, M. I. Kurkin, M. P. Petrov, and V. P. Chekmarev, Sov. Phys. Usp. **27**, 235 (1984).
[16] Yu. M. Bunkov, Sov. Phys. Usp. **53**, 843 (2010).
[17] T. Kunimatsu, T. Sato, K. Izumina, A. Matsubara, Y. Sasaki, M. Kubota, O. Ishikawa, T. Mizusaki, and M. Bunkov, JETP Lett. **86**, 216 (2007).
[18] J. Elbs, Yu. M. Bunkov, E. Collin, H. Godfrin, and G. E. Volovik, Phys. Rev. Lett. **100**, 215304 (2008).
[19] T. Sato, T. Kunimatsu, K. Izumina, A. Matsubara, M. Kubota, T. Mizusaki, and Yu. M. Bunkov, Phys. Rev. Lett. **101**, 055301 (2008).

[20] P. Hunger, Yu. M. Bunkov, E. Collin, and H. Godfrin, J. Low Temp. Phys. **158**, 129 (2010).

[21] Yu. M. Bunkov, E. M. Alakshin, R. R. Gazizulin, A. V. Klochkov, V. V. Kuzmin, T. R. Safin, and M. S. Tagirov, JETP Lett. **94**, 68 (2011); E. M. Alakshin, Yu. M. Bunkov, R. R. Gazizulin, A. V. Klochkov, V. V. Kuzmin, A. S. Nizamutdinov, T. R. Safin, and M. S. Tagirov, J. Phys. Conf. Ser. **324**, 012006 (2011).

[22] W. N. Hardy and L. A. Whitehead, Rev. Sci. Instrum. **52**, 213 (1981).

[23] V. E. Zakharov, V. S. L'vov, and G. E. Falkovich, *Kolmogorov Spectra of Turbulence, Wave Turbulence* (Springer-Verlag, Berlin, 1992), Vol. 1.

[24] S. O. Demokritov, V. E. Demidov, O. Dzyapko, G. A. Melkov, A. A. Serga, B. Hillebrands, and A. N. Slavin, Nature (London) **443**, 430 (2006).